Acta Neuropathologica Communications

RESEARCH

Open Access

Sinomenine alleviates neuroinflammation in chronic cerebral hypoperfusion by promoting M2 microglial polarization and inhibiting neuronal pyroptosis via exosomal miRNA-223-3p

Qu Yang[1,2,3,4], Qi Chen[3], Kai-Bing Zhang[3], Yu Liu[1,4], Jia-Cheng Zheng[3], Dong-Xia Hu[1,4*] and Jun Luo[1,2,4*]

Abstract

Chronic cerebral hypoperfusion (CCH) is a major contributor to vascular dementia, with neuroinflammation playing a central role in its pathogenesis. Sinomenine (SINO), a natural alkaloid derived from traditional Chinese medicine, has shown significant anti-inflammatory and neuroprotective properties. However, its efficacy and mechanism of action in CCH remain unclear. In this study, we established a CCH rat model through bilateral common carotid artery occlusion and administered 10 mg/kg of SINO daily. Behavioral tests demonstrated that SINO significantly improved cognitive and memory functions in CCH rats. Histological analysis revealed that SINO effectively reduced neuroinflammation and damage in the hippocampal CA1, CA3, and DG regions. Mechanistically, SINO promoted microglial polarization from the M1 to M2 phenotype, markedly inhibiting the release of pro-inflammatory cytokines, including IL-1β, IL-6, and TNF-α. Further exploration of its neuroprotective mechanism showed that exosomes from SINO-treated microglia were enriched with miRNA-223-3p, which suppressed NLRP3-mediated pyroptosis in neurons. While our findings highlight the therapeutic potential of SINO, further studies are needed to validate its safety and efficacy in diverse populations and chronic settings. In summary, this study not only demonstrates SINO's regulatory effect on microglial polarization in CCH but also unveils a novel neuroprotective mechanism through exosomal miRNA-223-3p delivery, providing a solid theoretical foundation for SINO's potential as a treatment for CCH.

Keywords Chronic cerebral hypoperfusion, Sinomenine, Exosomal microRNA, Microglial polarization, Neuroinflammation, Pyroptosis

*Correspondence:
Dong-Xia Hu
hudongxia5489@sina.com
Jun Luo
luojun1786@163.com
[1]Department of Rehabilitation Medicine, The Second Affiliated Hospital, Jiangxi Medical College, Nanchang University, Nanchang, Jiangxi 330006, China
[2]Jiangxi Province Key Laboratory of Precision Cell Therapy, Nanchang, Jiangxi 330006, China
[3]Jiangxi Medical College, Nanchang University, Nanchang, Jiangxi 330006, China
[4]The National Engineering Research Centre for Bioengineering Drugs and the Technologies, Institute of Translational Medicine, Nanchang University, Nanchang, Jiangxi 330006, China

Introduction

Chronic cerebral hypoperfusion (CCH) is a pathological condition characterized by a long-term reduction in blood supply to entire or localized regions of the brain due to various causes. This leads to insufficient cerebral blood flow and an inability to meet the metabolic demands of the brain, resulting in chronic brain injury and neurological dysfunction [2, 34]. CCH plays a pivotal role in the pathogenesis of vascular cognitive impairment (VCI), ultimately leading to the development of vascular dementia (VaD), which ranks as the second most prevalent form of dementia following Alzheimer's disease (AD) [26]. The main clinical symptoms include progressive memory impairment, cognitive dysfunction, behavioral changes, emotional instability, and sleepiness, which significantly impact patients and their families' daily lives [46, 49]. According to World Health Organization (WHO) statistics, the global population of people with dementia reached 55.2 million in 2019, and this number continues to increase due to the aging population, presenting a formidable challenge and heavy burden for society [3, 16, 47]. Therefore, it is crucial to develop effective treatment strategies for CCH-induced brain injury and neurological dysfunction that hold great clinical significance and social value.

Neuroinflammation plays a crucial role in the development of CCH, as pathological changes in the extracellular microenvironment release damage-associated molecular patterns (DAMPs), triggering local and systemic inflammatory reactions that result in stress and damage to neurons and glial cells [30, 35]. Microglia, which serve as resident brain macrophages, play a critical role in regulating inflammation. Following activation, microglia differentiate primarily into proinflammatory M1-type and anti-inflammatory M2-type microglia. M1 microglia secrete neurotoxic inflammatory cytokines, such as IL-6, IL-1β, and TNF-α, which lead to neuronal damage and even death, aggravating brain damage [17]. M2 microglia can secrete crucial anti-inflammatory cytokines, including IL-4, IL-10, and TGF-β, which are vital for mitigating nerve cell death, facilitating nerve regeneration, and promoting neurological function recovery [14, 29]. Recent research has demonstrated that regulating the polarization of microglia toward the M2 phenotype can alleviate neuroinflammation in CCH and play a neuroprotective role [6, 15, 54], providing a key strategy for effectively treating CCH-induced brain damage and neurological dysfunction.

Sinomenine (SINO), an isoquinoline alkaloid derived from the traditional Chinese medicine caulis sinomenii, exhibits pronounced anti-inflammatory and immunosuppressive effects [21, 23]. Recent research has demonstrated that SINO is neuroprotective in the nervous system [11]. By inhibiting the activation of microglia and astrocytes, as well as NLRP3 inflammasome activation, SINO reduces the release of inflammatory factors, thereby alleviating brain damage in ischemic stroke [32, 33], intracerebral hemorrhage [48], and AD [40]. However, the regulatory role of SINO in CCH-associated inflammation remains unclear. In this study, we discovered that SINO can regulate the polarization of microglia from the M1 to the M2 phenotype, suppress inflammation, and promote the secretion of beneficial cytokines. However, further investigation is necessary to explore its effects and pathways on neurons.

Importantly, the exosomes released by microglia are essential for enabling communication between microglia and neurons [1, 45]. Exosomes, small extracellular vesicles ranging in diameter from 40 to 160 nm, are secreted by various cell types. They can be endocytosed by adjacent or distant cells and facilitate the transportation of multiple biological components, including lipids, proteins, mRNAs, microRNAs (miRNAs), and other noncoding RNAs (ncRNAs) [43, 50]. Among them, the most widely studied is miRNA, which has been proven to play a crucial role in regulating various physiological and pathological processes of receptor cells in diverse diseases, including those affecting the central nervous system [19, 42]. Several studies have demonstrated that promoting microglial polarization toward the M2 phenotype leads to the release of exosomes, which are then taken up by neurons. The miRNAs carried in these exosomes can modulate downstream target genes to suppress neuroinflammation and neuronal death, thus mitigating ischemic stroke [41, 44, 52], craniocerebral trauma [10], and AD [5]. Therefore, we conducted a comprehensive study on the impact of exosomes released by microglia following SINO treatment on neurons and the involvement of exosomal miRNAs in this process.

In this study, we hypothesized that SINO could modulate microglial polarization from the M1 to the M2 phenotype and promote the secretion of exosomes containing anti-inflammatory miRNAs. When microglial exosomes are absorbed by neurons, these miRNAs exert neuroprotective effects by regulating the expression of downstream target genes or signaling pathways to mitigate neuroinflammation.

Our findings demonstrated that SINO facilitates the polarization of microglia from the M1 phenotype to the M2 phenotype and that the exosomes released by these cells exhibit high expression of miR-223-3p, which selectively targets *Nlrp3* after endocytosis by neurons. The NLRP3 protein, acting as a pivotal mediator of inflammation and pyroptosis, forms an inflammasome complex with ASC and pro-caspase-1. This complex activates caspase-1 to cleave pro-IL-1β, pro-IL-18, and gasdermin D (GSDMD), resulting in the generation of active IL-1β, IL-18, and the N-terminal fragment of gasdermin

D (GSDMD-N). Consequently, this process aggravates inflammatory responses and facilitates cell lysis [13, 37]. Afterward, miR-223-3p subsequently downregulated the expression of *Nlrp3* and inhibited the activation of the NLRP3 inflammasome, thereby attenuating neuroinflammation and pyroptosis. Ultimately, this effectively alleviated brain injury and cognitive dysfunction after CCH.

This study emphasizes the key role of SINO in regulating microglial polarization and exosome secretion to mediate neuroinflammation and pyroptosis in CCH, providing a theoretical basis for the use of SINO in the treatment of CCH-induced brain injury and neurological dysfunction.

Materials and methods

Animals

SPF-grade male Sprague–Dawley rats (6 weeks old, weighing 180–200 g) were obtained from Tianqin Biotechnology Co., Ltd. (Changsha, China). The rats were housed at an appropriate temperature and humidity and under a 12-hour light/dark cycle at the Circulatory Standardized Animal Experiment Center. Water and food are freely available. All animal experiments were carried out under the guidelines of the Animal Care and Use Committee of Nanchang University (China) and followed the Guide for the Care and Use of Laboratory Animals of the National Institutes of Health.

CCH rat model and drug administration

In this study, we used rats with bilateral common carotid artery occlusion (BCCAO) to establish a CCH animal model and treated them with SINO (GN10054, Glpbio, USA). The flowchart is shown in Fig. 1A. After one week of adjustable feeding, the rats were randomly divided into the following 3 groups: (1) the sham group, (2) the CCH group, and (3) the CCH + SINO group, $n = 10$ per group. The surgical procedure was performed based on previous research [46]. All rats were fasted before the surgery. 1% pentobarbital sodium (30 mg/kg) was intraperitoneally injected to induce anesthesia. The rats were fixed in the supine position and routinely disinfected. The skin was incised along the midline of the neck, precisely at its intersection with the clavicle. Moreover, the skin, fascia, muscle, and vagus nerve were dissected layer by layer. When the common carotid artery and vagus nerve were exposed, the vagus nerve was carefully separated with a glass nerve dissector to avoid pulmonary edema caused by traction. Then, the common carotid arteries were exposed and separated, 4–0 threads were ligated, one side was ligated first, the other side was ligated three days later, and the 0th thread was sutured. In the sham group, anesthesia and layer-by-layer separation were also performed without ligation of the common carotid artery. Electric blankets were used for insulation throughout the operation. The day following the surgical procedure, the rats in the CCH + SINO group were treated with SINO (10 mg/kg). SINO was injected intraperitoneally (i.p.) every day for two weeks. The sham and CCH groups were treated with normal saline.

Morris water maze (MWM) test

The MWM test was used to assess learning and memory ability [8]. The installation is a black pool with a diameter of 1.6 m and a height of 0.5 m divided into four quadrants, with the water temperature controlled at 20 ± 1 °C. Visual cues are set in each quadrant direction, while black curtains surround the pool to prevent external visual interference. A platform with a diameter of 9.5 cm was fixed in the fourth quadrant and submerged 1 cm below the water surface. A video tracking system was installed above the pool to record the rats' movement tracks.

The experiment consisted of two phases: the platform hidden period was used to assess spatial learning ability, while the platform removal period was used to evaluate spatial memory ability. (1) Platform hidden experiment. From days 1 to 5, the rats were placed in the pool from four quadrants facing the pool wall and allowed to freely search for the platform for 60 s. If they landed successfully, the time was recorded as the escape latency. They were guided to the platform if they failed, and their escape latency was recorded as 60 s. Subsequently, they were permitted to remain on the platform for 15 s. (2) The probe trial was performed on day 6. The platform was removed during the experimental period. The platform was removed, and the rats were placed into the water from the diagonal quadrant of the platform. The mice were allowed to explore for 60 s. The test was conducted only once, and the following indicators were recorded: the number of platform crossings, average swimming speed, duration, and percentage of time spent in the target quadrant ($n = 5$ per group).

Fixation of brain tissue

After the behavioral test, the rats were anesthetized by intraperitoneal injection of 2% pentobarbital sodium (45 mg/kg), and the heart was fully exposed through thoracotomy. A perfusion needle was inserted into the apex of the rat heart, which was aligned parallel to the heart's vertical axis. Approximately 100–200 mL of 0.9% cold saline was injected until the outflow fluid was clarified, and 4% paraformaldehyde was used to continue the infusion until the rats became stiff in rapid sequence. Finally, the brain was removed by decapitation and fixed in 4% paraformaldehyde for histological or immunohistochemical detection.

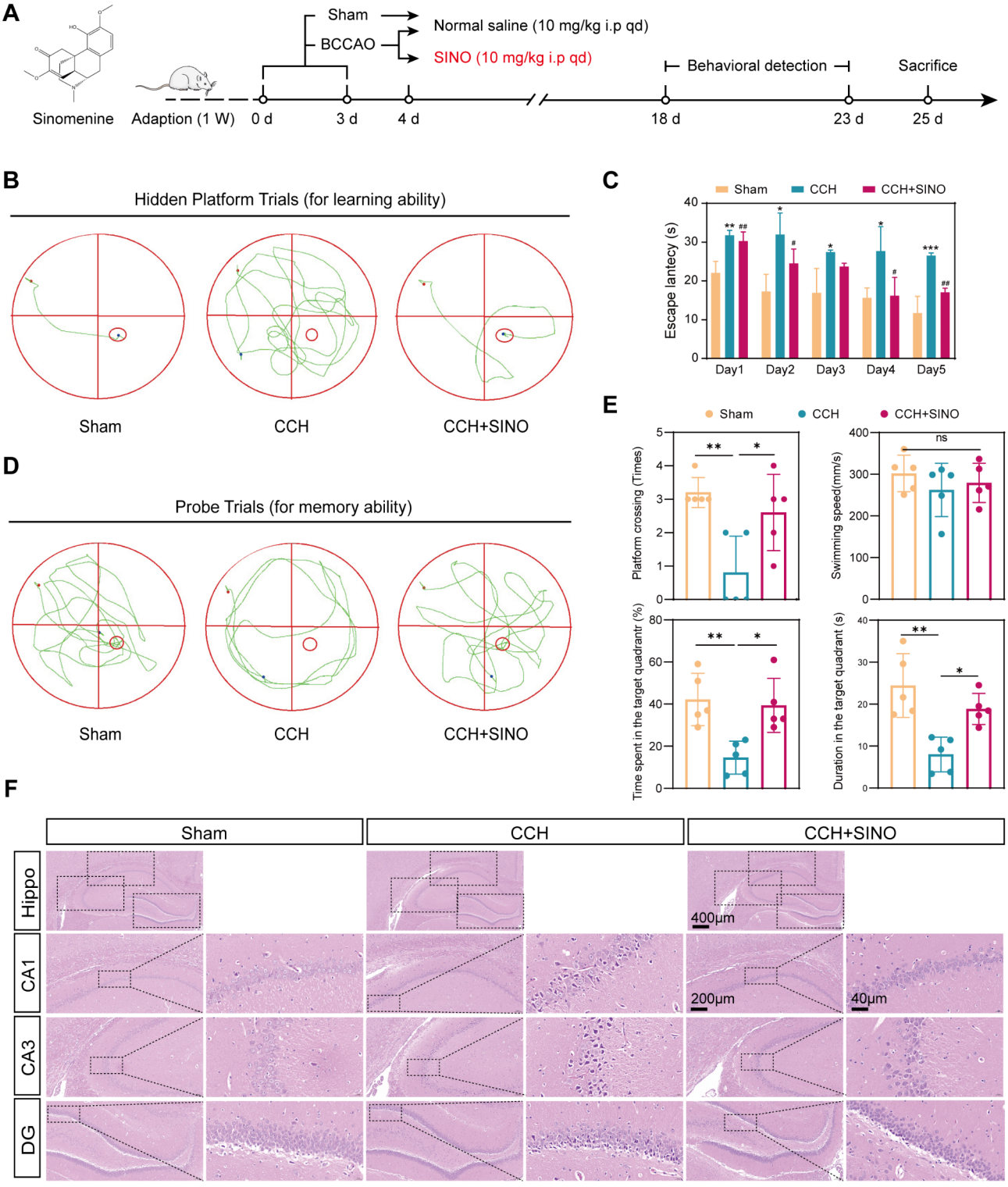

Fig. 1 Assessment of the effects of sinomenine (SINO) treatment on rat brain injury and cognitive function. (**A**) Flowchart showing the construction of the CCH rat model and treatment process with SINO. (**B**, **C**) The Morris water maze (MWM) test of the hidden platform was conducted from day 1 to day 5 to evaluate the learning ability of the rats. The escape latency refers to the time it takes for rats to find the platform. (**D**, **E**) The probe trial on the sixth day of the MWM test was used to assess the memory ability of the rats ($n = 5$ per group). (**F**) Observation of brain tissue damage via hematoxylin and eosin staining. $^{ns}P > 0.05$, $^{*}P < 0.05$, $^{**}P < 0.01$, and $^{***}P < 0.001$ vs. the Sham group. $^{\#\#}P < 0.01$ vs. the CCH group

Immunostaining

Brain tissue sections were dewaxed, rehydrated, and stained with hematoxylin and eosin (HE) for histological analysis. Light microscopy was used to observe the histomorphology of the neurons. For immunofluorescence staining, 5 μm thick sections were prepared and incubated with blocking buffer (10% goat serum and 0.5% Triton X-100 in phosphate-buffered saline) at room temperature for 1 h. Then, the sections were incubated with the following primary antibodies overnight at 4 °C: rabbit anti-IBA1 (1:500, 10904-1-AP, Proteintech), rabbit anti-INOS (1:500, 80517-1-RR, Proteintech), rabbit anti-NLRP3 (1:500, 19771-1-AP, Proteintech) and rabbit anti-GSDMD (1:500, 20770-1-AP, Proteintech). After being washed three times in phosphate-buffered saline with Tween-20, the secondary antibody (1:200, SA00013-2 and SA00013-4, Proteintech) was used for the reaction at room temperature for 1 h in the dark. Finally, after the cells were subjected to DAPI treatment, fluorescence images after staining were obtained under a microscope. The analysis was performed using ImageJ, with the intensity values were normalized by dividing by the total area of the hippocampus to account for variations in brain, and all measurements were taken from the same bregma coordinates, $n = 3$ per group.

Microglial cell culture and treatments

Rat microglia (RM) cells (ScienCell, California, USA) were cultured in Dulbecco's modified Eagle's medium (DMEM) supplemented with 10% FBS and 100 g/L penicillin/streptomycin in an incubator at 37 °C with 5% CO_2 saturated humidity. The cells were digested with 0.25% trypsin and passaged to the logarithmic stage for the experiments. To establish the RM cell inflammation model, we exposed RM cells to 1 μg/mL lipopolysaccharide (LPS) for various predetermined durations (2, 4, and 8 h) [36]. The experimental concentrations and treatment times were determined based on significant differences. RM cells were treated with different concentrations (0, 0.05, 0.1, 0.2, 0.4, 0.8, 1, 2, and 4 μM) of SINO for 24 h. The final experimental concentration was determined through CCK-8 assays, where we selected a concentration that showed a significant difference in cell viability. To detect the anti-inflammatory effect of SINO on RM cells, the cells were divided into three groups: the control group, in which the cells were cultured normally; the LPS group, in which the cells were treated with LPS for 4 h; and the LPS + SINO group, in which the cells were treated with SINO after being exposed to LPS.

Cell viability assays

A Cell Counting Kit-8 (CCK-8, Beyotime, China) assay was used to assess cell viability according to the manufacturer's instructions. When the RM cells had reached 80% confluence, they were digested with 0.25% trypsin for 2 min, and the reaction was terminated with a medium supplemented with serum. The cells were collected by centrifugation at 1000 rpm for 5 min, resuspended, and seeded in 96-well plates at approximately 5×10^3 cells/well. After treatment with LPS or SINO, 10 μL of CCK-8 solution was added to each well, and the cells were incubated in an incubator for 2 h. The optical density (OD) value was determined at 450 nm using a microplate reader.

Flow cytometry

Flow cytometry was used to detect the phenotypes of CD86 + and CD206 + microglia. The cells from each group were collected. The viable cells were counted, resuspended in cell staining buffer (420201, BioLegend, USA) at $5–10 \times 10^6$ cells/mL, and 100 μl/tube of cell suspension ($5–10 \times 10^5$ cells/tube) was distributed into 12 × 75 mm plastic tubes. A cocktail of fluorochrome-conjugated APC-CD86 (200316, BioLegend) and PE-CD206 (141706, BioLegend) in combination with Fc Receptor Blocking Solution (422301, BioLegend) was added for 30 min at 4 °C in the dark. The cells were washed twice with at least 2 mL of cell staining buffer by centrifugation at 350× g for 5 minutes. The cell pellet was resuspended in 0.5 ml of cell staining buffer, and 5 μl (0.25 μg)/million cells of 7-AAD viability staining solution (420403, BioLegend) were added to exclude dead cells. Dead cells are labeled with the 7-ADD dye, whereas live cells remain unlabeled. The mixture was incubated for 3–5 minutes at 4 °C in the dark. Flow cytometric analysis was performed to determine the frequency of positively stained cells and the geometric mean fluorescence intensity (MFI). To calculate the proportion of microglial cells that are positive for CD86 or CD206 in live cells, we used the following formula: positive cell ratio = (CD86 + or CD206 + without 7-AAD) / (CD86- or CD206- without 7-AAD) × 100%.

Conditioned medium derived from RM cells treats H_2O_2-induced injury in PC12 cells

To investigate the effects of exosomes derived from microglia on neuronal injury, we collected the supernatant of RM cells from different groups as conditioned mediums (RM-CM) to treat hydrogen peroxide (H_2O_2)-treated PC12 cells. The experimental groups included the control group, LPS group, LPS + SINO group, and LPS + SINO + GW4869 group. GW4869 (567715, Merck), a sphingomyelinase inhibitor, is widely used as an exosome inhibitor. To establish neuronal injury, we treated PC12 cells with 100 μM H_2O_2 for 24 h. Afterward, we removed the supernatant and treated the cells with RM-CM from the respective groups for another 24 h to explore the effects of exosomes from RM cells on

neuronal injury. The PC12 cells were collected for subsequent validation.

Isolation and identification of RM exosomes (RM-Exos)

Healthy RM cells were divided into two culture dishes. The following day, the cells were treated with 1 μg/mL LPS for 4 h. Subsequently, the cells were treated with or without SINO for 24 h. The supernatant was collected from both culture dishes, and an exosome extraction and purification kit (UR52121, Umibio, Shanghai) was used according to the manufacturer's instructions to isolate the exosomes. The two groups were designated CON-RM-Exos and SINO-RM-Exos, respectively. Transmission electron microscopy was used to observe the morphology of the exosomes, and a nanoparticle tracking analyzer was used to detect and analyze the size distribution of the exosomes. Approximately 1.5E + 10 exosomes can be extracted from 20 mL of SINO-treated RM cell culture supernatant, which are then dissolved in 200 μL of PBS for treatment of H_2O_2-treated PC12 neuronal cells. According the Exosome Protein Detection Kit (UR52301, Umibio), 20 μg of exosomes were used to detect the expression of the exosome marker CD63 and CD81 by Western blotting.

miRNA microarray analysis

OE Biotechnology Co., Ltd. (Shanghai, China) conducted miRNA microarray analysis and RM exosome data analysis. The exosome pellet was lysed using TRIzol reagent (#15596018, Thermo Fisher). After phase separation with chloroform, the aqueous phase containing RNA was collected and RNA was precipitated with isopropanol. The RNA pellet was washed with 75% ethanol and then dissolved in nuclease-free water. Total RNA was quantified with a NanoDrop ND-2000 (Thermo Scientific), and RNA integrity was assessed with an Agilent Bioanalyzer 2100 (Agilent, USA). The labeling of the samples, microarray hybridization, and washing were carried out following the standard protocols provided by the manufacturer. Briefly, total RNA was dephosphorylated, denatured, and then labeled with Cyanine-3-CTP. Following purification, the RNAs were subjected to microarray hybridization with 780 probes for mature miRNA. After washing, the arrays were scanned with an Agilent G2505C scanner (Agilent, USA). Feature Extraction software (version 10.7.1.1, Agilent) was used to analyze the array images to obtain the raw data. Differentially expressed miRNAs were identified based on the fold change (≥ 2.0) and P value (≤ 0.05) calculated using a t-test and validated by RT–qPCR. The selected miRNAs were subjected to further analysis to determine their functions.

Target prediction and transfection of miR-223-3p

Target prediction for miR-223-3p was conducted using TargetScan (http://targetscan.org/) and miRDB (http://mirdb.org/miRDB/). To investigate the function of RM exosomal miR-223-3p, we transfected RM cells with miR-223-3p mimics (miR10000892-1-5, RiboBio, China) and inhibitors (miR20000892-1-5, RiboBio). According to the instructions, the transfection complex was prepared, and the concentration of the miR-223-3p mimic was adjusted to 50 nM, while that of the miR-223-3p inhibitor was adjusted to 100 nM. Then, the solution was added to DMEM without penicillin-streptomycin. The transfection solution was added to the RM cells when the cell density reached 30–50%. After culture in a CO_2 incubator at 37 °C for 48 h, the supernatant was collected to isolate the exosomes. RT–qPCR was used to detect the expression of exosomal miR-223-3p to verify the transfection efficiency of the mimic and inhibitor. Subsequently, H_2O_2-treated PC12 cells were treated with exosomes from each transfected group for 24 h, and *Nlrp3* mRNA expression levels were detected by RT–qPCR. Furthermore, to investigate whether SINO-RM-Exos exert their effects through miR-223-3p, H_2O_2-induced PC12 cells were treated with SINO-RM-Exos, with or without the miR-223-3p inhibitor, for 24 h. The cells were then collected for subsequent experiments.

Quantitative real-time polymerase chain reaction (RT–qPCR)

Total RNA was isolated from brain tissues, cells, and exosomes using RNAkey™ Reagent (SM129-02, Sevenbio, China). The RNA of tissues and cells was reverse transcribed to synthesize cDNA using an All-in-one First Strand cDNA Synthesis Kit III (SM135, Sevenbio). The exosomal miRNAs were reverse transcribed to synthesize cDNA using a SweScript RT II First Strand cDNA Synthesis Kit (G3333, Servicebio, China). Subsequently, 2× SYBR Green qPCR Master Mix II (SM143, Sevenbio) was used for quantitative PCR (qPCR) following the manufacturer's instructions. All primer sequences are listed in Table S1.

Western blot

Total protein was extracted from brain tissues and cells using RIPA lysis buffer, quantified with a BCA Protein Assay Kit (PC0020, Solarbio, China), subjected to SDS–PAGE electrophoresis, and transferred to a PVDF membrane. The membrane was blocked with 5% skim milk for 1.5 h at room temperature, followed by overnight incubation with diluted primary antibody at 4 °C. After that, the membrane was incubated with horseradish peroxidase-conjugated secondary antibodies for 1 h at room temperature. The secondary antibodies used were from Proteintech, chosen based on the species of the

primary antibody. Protein levels were assessed in various samples using enhanced chemiluminescence (ECL) and quantified by ImageJ after washing three times with Tris-buffered saline containing Tween-20. Unless otherwise specified, all the following antibodies were purchased from Proteintech: NLRP3 (1:2000, 19771-1-AP), ASC (1:2000, 10500-1-AP), CASP1 (1:2000, 22915-1-AP), GSDMD (1:2000, 20770-1-AP), IL-1β (1:2000, 26048-1-AP), IL-18 (1:2000, 10663-1-AP), CD206 (1:1000, 18704-1-AP), INOS (1:1000, 18985-1-AP), and GAPDH (1:5000, 10494-1-AP).

Statistical analysis

All the experiments were repeated at least three times. Quantitative data are shown as the mean ± standard deviation. Student's t-test was used to analyze significant differences between two groups, and analysis of variance (ANOVA) was used to evaluate the differences between multiple groups. When the assumption of homogeneity of variance was met, the Bonferroni post-hoc test was applied following ANOVA. For non-parametric data, the Kruskal-Wallis test was used. A p-value of < 0.05 was considered statistically significant.

Results

SINO alleviated brain injury and improved learning and memory in CCH rats

According to the process outlined in Fig. 1A, a CCH rat model was constructed, and the therapeutic effect of SINO was evaluated. The Morris water maze (MWM) was used to evaluate the enhancement of spatial learning and memory ability in CCH rats treated with SINO. At the end of the animal experiment, the rats were euthanized, and brain samples were collected for subsequent testing. As shown in Fig. 1B and C, both the Sham group and the CCH + SINO group outperformed the CCH group in locating the platform. Despite the decreasing trend in escape latency for all groups during hidden platform training, the CCH group consistently exhibited longer escape latency than the Sham and CCH + SINO groups. Compared to the CCH group, the CCH + SINO group exhibited a significantly shorter escape latency, particularly on the 4th and 5th days. Furthermore, the memory ability of the rats is illustrated in Fig. 1D and E. Rats in the CCH + SINO and Sham groups frequently crossed the platform, while those in the CCH group circled the pool wall. Both the CCH + SINO group and the Sham group exhibited a longer duration and greater percentage of time spent in the target quadrant than did the CCH group. It is important to note that there was no significant difference in the swimming speed of each group, indicating that the differences in escape latency are not affected by swimming ability. The MWM results indicated that CCH rats induced by BCCAO exhibited a significant decrease in spatial learning and memory ability, but SINO treatment significantly improved their performance. HE staining were performed on the hippocampus of the rats (Fig. 1F). Neurons in the CA1, CA3, and dentate gyrus (DG) regions displayed normal morphology, orderly arrangement, and distinct cell nuclei in the sham operation group. In contrast, the CCH group exhibited pathological changes such as nuclear condensation and increased staining intensity. However, SINO treatment effectively alleviated these pathological changes (Fig. 1F). Furthermore, we conducted an in vivo biosafety assessment of SINO. HE staining revealed no significant damage to the heart, liver, spleen, lungs, or kidneys following SINO treatment (Table S2). There were no notable differences in blood indicators, such as aspartate aminotransferase (AST), total bilirubin (TBIL), direct bilirubin (DBIL), uric acid (UA), creatinine (CREA), or blood urea nitrogen (BUN) levels, indicating that SINO treatment did not adversely affect liver and kidney functions or cause any systemic toxicity (Table S3). Taken together, these results suggested that treatment with SINO effectively prevented cognitive dysfunction and neuronal injury in CCH rats.

SINO reduces neuroinflammation and promotes M2 polarization of microglia in the hippocampus of CCH rats

Microglia, the resident immune cells of the central nervous system, play a critical role as the responder to injury with in the brain. The hippocampus is a vital brain structure responsible for learning and memory processes. As shown in Fig. 2A and B, ionized calcium-binding adapter molecule 1 (IBA1), a specific protein marker for microglial activation, exhibited strong positivity in the hippocampus of rats in both the CCH group and CCH + SINO group, whereas it was not pronounced in the Sham group. Compared to those in the CCH group, the levels of IBA1 protein decreased in the CCH + SINO group. This finding suggested that there was damage and an inflammatory response in the hippocampus of BCCAO-induced CCH rats, leading to the recruitment and activation of microglia, while SINO treatment partially alleviated this response.

However, as IBA1 cannot determine the polarization type of microglia, we detected M1- and M2-specific markers of microglia. The PCR results revealed that the M1-type marker genes *Inos*, *IL-1β*, and *IL-18* were highly expressed in the CCH group, while they exhibited low expression in the CCH + SINO group. Conversely, the M2-type marker genes *Arg1*, *IL-4*, and *IL-10* exhibited low expression in the CCH group but high expression in the CCH + SINO group (Fig. 2C). WB analysis revealed an increase in the level of INOS protein and a decrease in the level of ARG-1 protein in the CCH group, while the opposite trend was observed in the CCH + SINO group

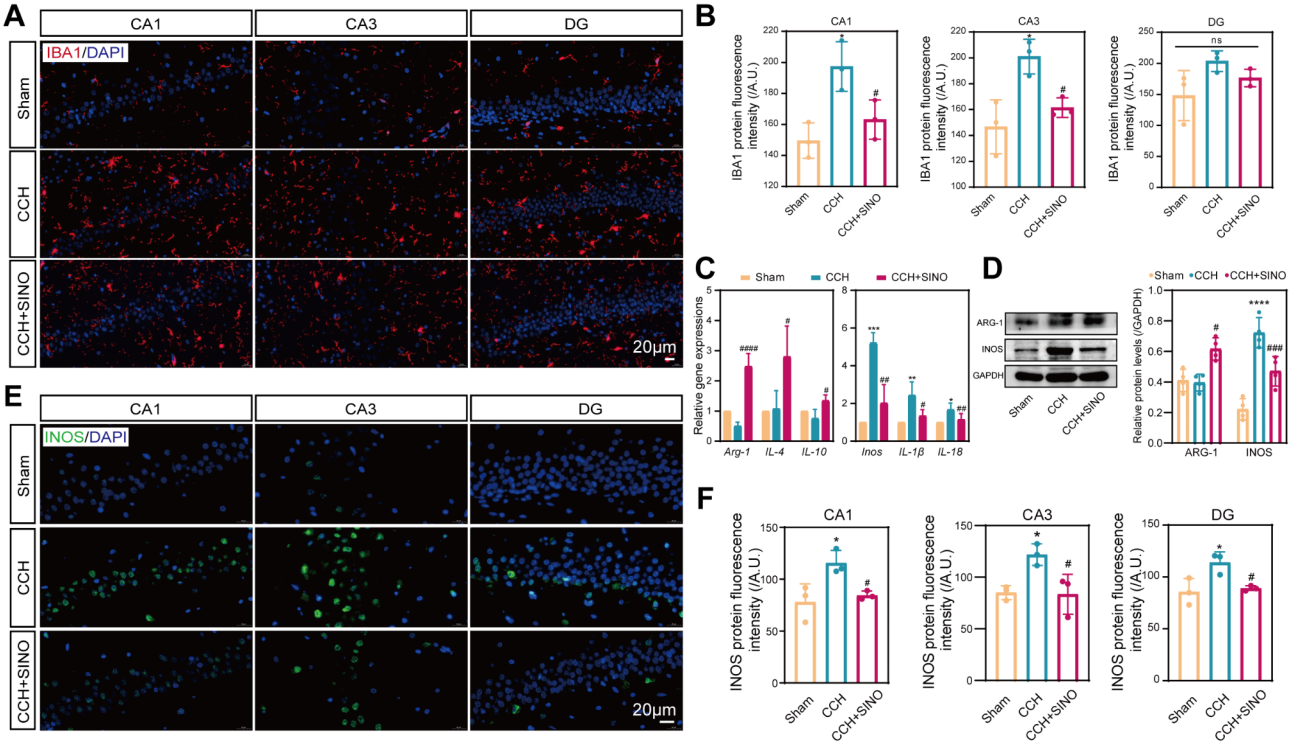

Fig. 2 Effects of SINO treatment on neuroinflammation and microglial polarization in the brain tissue of CCH rats. (**A**, **B**) Immunofluorescence was used to assess and quantify the expression levels of the activated microglial marker protein IBA1 in the hippocampal region of the rat brain. The results are expressed as the fluorescence intensity of each arbitrary unit. (**C**) RT-qPCR analysis was conducted to examine the expression of M1-type genes, including *Inos*, *IL-1β*, and *IL-18*, and the expression of M2-type genes, including *Arg-1*, *IL-4*, and *IL-10*. (**D**) Western blot (WB) analysis was conducted to evaluate the levels of the M1-type protein INOS and the M2-type protein ARG-1 ($n = 4$ per group). (**E**, **F**) The levels of INOS protein in the CA1, CA3, and DG regions of the brain were measured using immunofluorescence. $^{ns}P > 0.05$. $^{*}P < 0.05$, $^{**}P < 0.01$, and $^{***}P < 0.001$ vs. the Sham group. $^{\#}P < 0.05$, $^{\#\#}P < 0.01$, and $^{\#\#\#\#}P < 0.0001$ vs. the CCH group

(Fig. 2D). Moreover, the immunofluorescence results showed strong positivity of the INOS protein in the CA1, CA3, and DG regions of CCH rats, which was significantly weakened after treatment with SINO (Fig. 2E and F). These findings indicate that CCH induces brain injury and inflammatory responses, leading to the activation of M1-type microglia and promoting inflammation; however, SINO treatment can regulate M2-type microglial polarization and help suppress inflammation.

SINO prevented CCH-induced NLRP3-mediated neuronal pyroptosis

Next, we further examined the influence of inflammation on neuronal pyroptosis. As depicted in Fig. 3A-D, there was a significant increase in the fluorescence positivity of the NLRP3 and GSDMD proteins in the CA1, CA3, and DG regions of rats in the CCH group compared to those in the Sham group. However, within the CCH + SINO group, there was a decrease in the fluorescence of these proteins relative to that in the CCH group. Subsequent WB analysis revealed that the levels of NLRP3, ASC, CASP1, and GSDMD-N were significantly greater in the CCH group than in the CCH + SINO group and Sham group (Fig. 3E-I). Additionally, the ratios of IL-1β/pro-IL-1β and IL-18/pro-IL-18 were increased in the CCH group but decreased in the CCH + SINO group (Fig. 3J and K). Furthermore, the PCR results indicated that *Nlrp3* and *Gsdmd* gene expression was significantly upregulated in CCH rats compared to sham rats but inhibited in CCH + SINO rats (Fig. 3L and M). These findings suggest that inflammation induces NLRP3-mediated pyroptosis in CCH rats and that SINO treatment has a notable inhibitory effect on this process.

SINO suppresses the LPS-induced inflammatory response in RM cells and enhances their M2 polarization

According to previous research, we selected LPS to induce an in vitro inflammatory microenvironment in RM cells. The process of cell grouping and treatment is shown in Fig. 4A [36]. A concentration of 1 μg/mL and treatment time of 4 h was determined through cell viability analysis (Fig. 4B). Moreover, we treated the cells with 0.5 μM of SINO for 24 h in subsequent experiments (Fig. 4C). As depicted in Fig. 4D, the gene expression levels of *IL-1β*, *TNF-α*, *IL-6*, and *IFN-γ* were significantly increased following LPS treatment, whereas they were

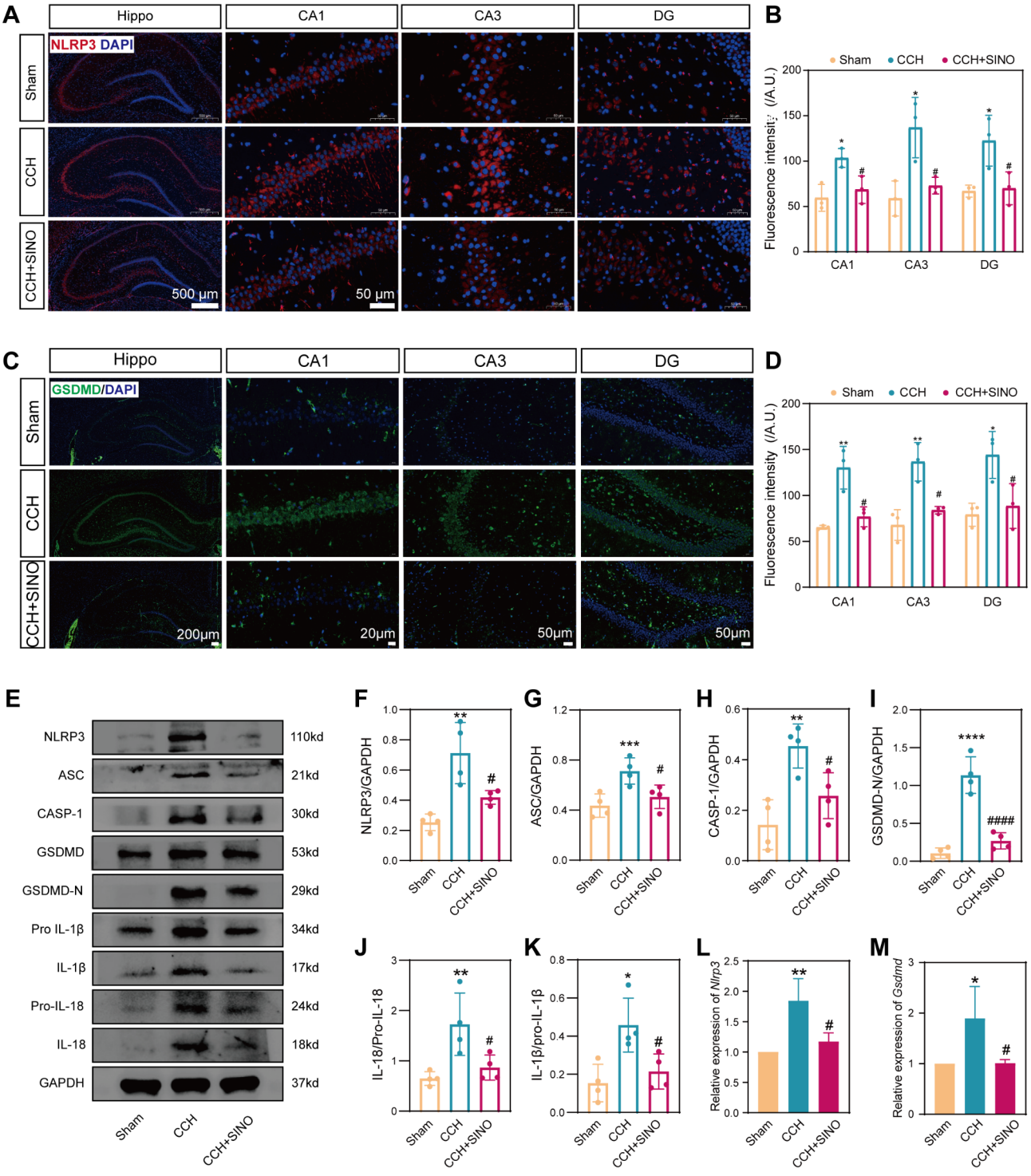

Fig. 3 Effects of SINO treatment on neuronal pyroptosis in CCH rats. (**A**-**D**) Immunofluorescence was used to measure the levels of the pyroptosis-related proteins NLRP3 and GSDMD. (**E**-**K**) Further analysis of the levels of proteins downstream of NLRP3 via WB analysis. (**L**, **M**) RT–qPCR was used to verify the mRNA expression of *Nlrp3* and *Gsdmd*. $^{*}P < 0.05$, $^{**}P < 0.01$, $^{***}P < 0.001$ vs. the Sham group. $^{\#}P < 0.05$ vs. the CCH group. $n = 4$ per group

markedly decreased after SINO treatment. This finding suggested that SINO effectively suppresses LPS-induced cellular inflammation. Furthermore, in the LPS group, the M1 marker gene *Inos* exhibited high expression, while the M2 marker gene *Arg-1* showed low expression; this pattern was reversed in the LPS + SINO group (Fig. 4E). These findings were further confirmed by immunofluorescence staining and WB analysis. Immunofluorescence

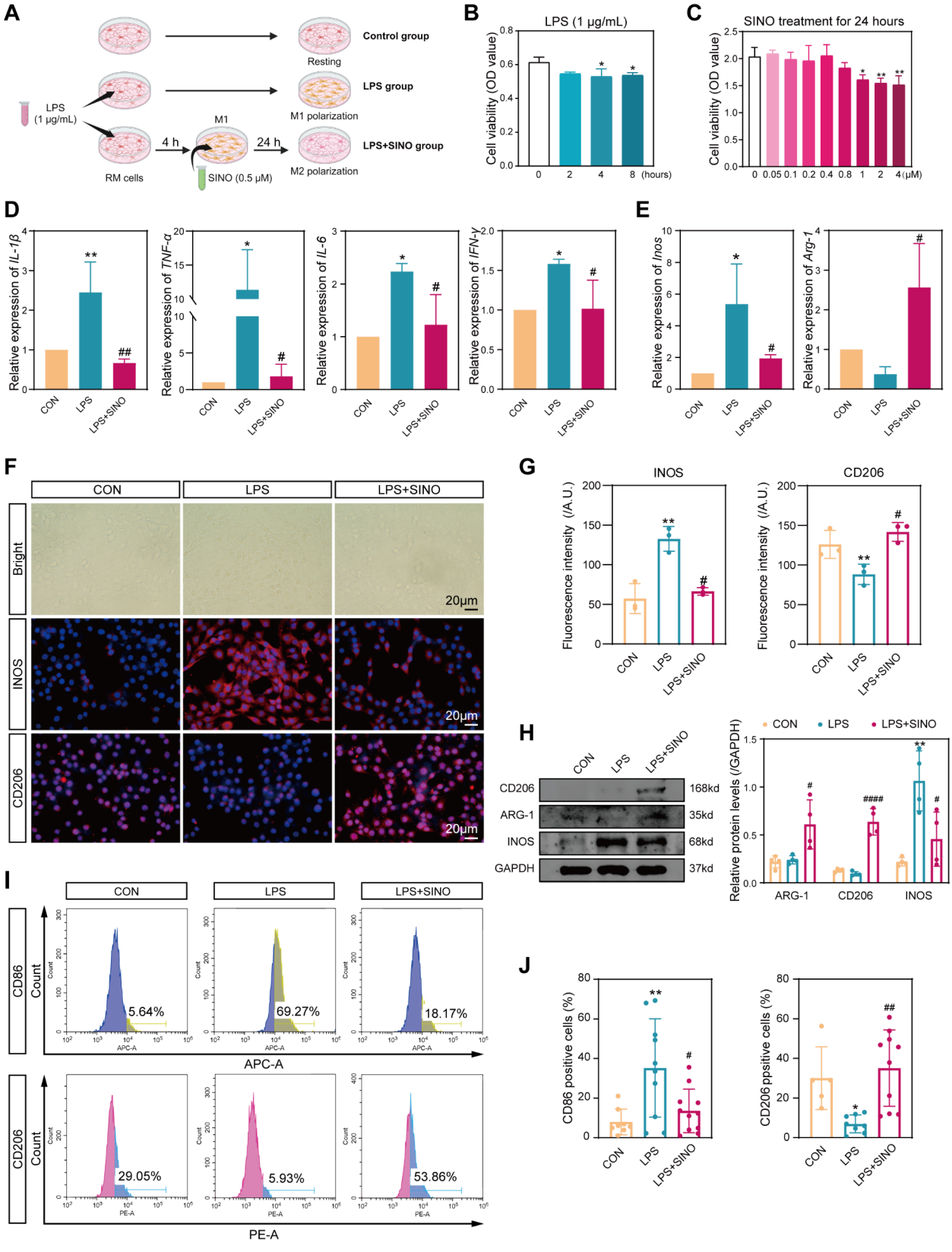

Fig. 4 (See legend on next page.)

(See figure on previous page.)

Fig. 4 In vitro, SINO regulates inflammation and polarization in LPS-induced RM cells. (**A**) Schematic diagram showing the establishment of an inflammation model in RM cells and treatment with SINO. (**B**, **C**) The effects of LPS and SINO dosages on RM cell viability were assessed by the CCK-8 assay. (**D**) RT–qPCR analysis of the mRNA expression of inflammatory markers, including *IL-1β*, *TNF-α*, *IL-6*, and *IFN-γ*, in RM cells. (**E**) Expression levels of the M1-type marker gene *Inos* and the M2-type marker gene *Arg-1* in RM cells. (**F**, **G**) Immunofluorescence observation and quantification of INOS and CD206 protein levels in RM cells. (**H**) WB analysis of the levels of the M1-type marker protein INOS and the M2-type marker proteins ARG-1 and CD206 in RM cells ($n = 4$ per group). (**I**, **J**) Flow cytometry analysis of the protein levels of the surface markers CD86 and CD206 in RM cells. $^{*}P < 0.05$ and $^{**}P < 0.01$ vs. the control group. $^{\#}P < 0.05$, $^{\#\#}P < 0.01$, and $^{\#\#\#\#}P < 0.0001$ vs. the LPS group

also revealed a significant reduction in INOS protein enrichment and an increase in ARG-1 protein enrichment after SINO treatment (Fig. 4F and G). WB analysis demonstrated that the LPS + SINO group exhibited decreased INOS protein levels and increased CD206 and ARG-1 levels compared to those in the LPS group (Fig. 4H). In addition, flow cytometry revealed differences in the surface markers of different cell types. In the LPS group, CD86 expression increased, while CD206 expression decreased; however, this trend was reversed in the LPS + SINO group (Fig. 4I and J). Overall, these results indicate that SINO can effectively suppress the inflammatory response of LPS-induced RM cells and facilitate their polarization from the M1 phenotype to the M2 phenotype.

Conditioned medium from SINO-treated RM cells prevents H_2O_2-induced pyroptosis in PC12 cells

Further investigation was conducted to examine the effects of RM cell supernatant on PC12 cells. As depicted in Fig. 5A, the supernatants from the control, LPS, and LPS + SINO groups of RM cells were collected as a conditioned medium to continue treating the PC12 cells for 24 h, followed by subsequent experimental detection and analysis. The viability of PC12 cells decreased after treatment with 100 μM of H_2O_2 (Fig. 5B). The addition of LPS-treated RM-CM further reduced PC12 cell viability, while SINO-treated RM-CM improved cell viability (Fig. 5C). Immunofluorescence analysis revealed an increase in the fluorescence of the NLRP3, ASC, and GSDMD proteins following H_2O_2 treatment compared to that in the untreated group. No significant change was observed after the addition of CM from the control RM cells. However, the fluorescence intensity further increased after the addition of CM from LPS-treated RM cells, while it significantly decreased after the addition of CM from LPS + SINO-treated RM cells (Fig. 5D). The WB results showed that the protein levels of NLRP3, ASC, CASP1, and GSDMD-N in H_2O_2-treated PC12 cells were significantly greater than those in untreated cells and further increased after culture with CM from LPS-treated RM cells (Fig. 5E-I). The ratios of GSDMD-N/GSDMD, IL-1β/pro-IL-1β, and IL-18/pro-IL-18 also exhibited similar trends (Fig. 5J-L). This indicates that H_2O_2 induces pyroptosis in PC12 cells, which is further exacerbated in the supernatant of LPS-treated RM cells. Treatment with CM from control RM cells did not decrease the levels of pyroptosis-related proteins; however, treatment with CM from LPS + SINO-treated RM cells significantly reversed the changes in the levels of these proteins. Moreover, the PCR results revealed that LPS + SINO-treated RM-CM significantly suppressed the expression of *Nlrp3* and *Gsdmd* (Fig. 5M and N). In conclusion, these findings suggest that compared to the control or LPS-treated RM cell supernatant, SINO treatment can effectively alleviate H_2O_2-induced PC12 cell damage and inhibit pyroptosis.

Exosomes derived from SINO-treated RM cells protected PC12 cells against pyroptosis

To investigate the impact of SINO-treated RM cell exosomes on PC12 cells, we cotreated RM cells with GW4869 to inhibit exosome secretion and collected the supernatant to treat H_2O_2-treated PC12 cells (Fig. 6A). As expected, immunofluorescence revealed that the fluorescence of the NLRP3, ASC, and GSDMD proteins in PC12 cells was enhanced after H_2O_2 induction, while treatment with LPS + SINO-treated RM-CM significantly weakened the fluorescence of these proteins. However, this protective effect was attenuated after cotreatment with GW4869 (Fig. 6B). Western blot analysis revealed a similar trend (Fig. 6C). Treatment with LPS + SINO-treated RM-CM reduced H_2O_2-induced increases in the levels of NLRP3, ASC, and GSDMD-N, but these effects were reversed by GW4869 (Fig. 6D-F). Therefore, these findings suggest that exosomes derived from RM cells treated with SINO play a crucial role in safeguarding PC12 cells against pyroptosis.

Exosomal mir-223-3p mediates the protective effects of SINO-activated microglia on neuronal pyroptosis

To further explore the mechanisms by which RM exosomes exert neuroprotective effects, we isolated exosomes and conducted miRNA sequencing analysis (Fig. 7A). Exosomes were categorized into two groups based on their source: those derived from RM cells treated with LPS alone (LPS-RM-Exos) and those derived from RM cells treated with both LPS and SINO (SINO-RM-Exos). Identification of the exosomes was performed using transmission electron microscopy, nanoparticle tracking analysis, and WB analysis. The exosomes exhibited a typical cup-shaped membrane vesicle morphology with diameters ranging from 40 to 160 nm (Fig. 7A and B). WB analysis confirmed the positive expression of the exosomal markers CD63 and CD81 (Fig. 7C). A total of

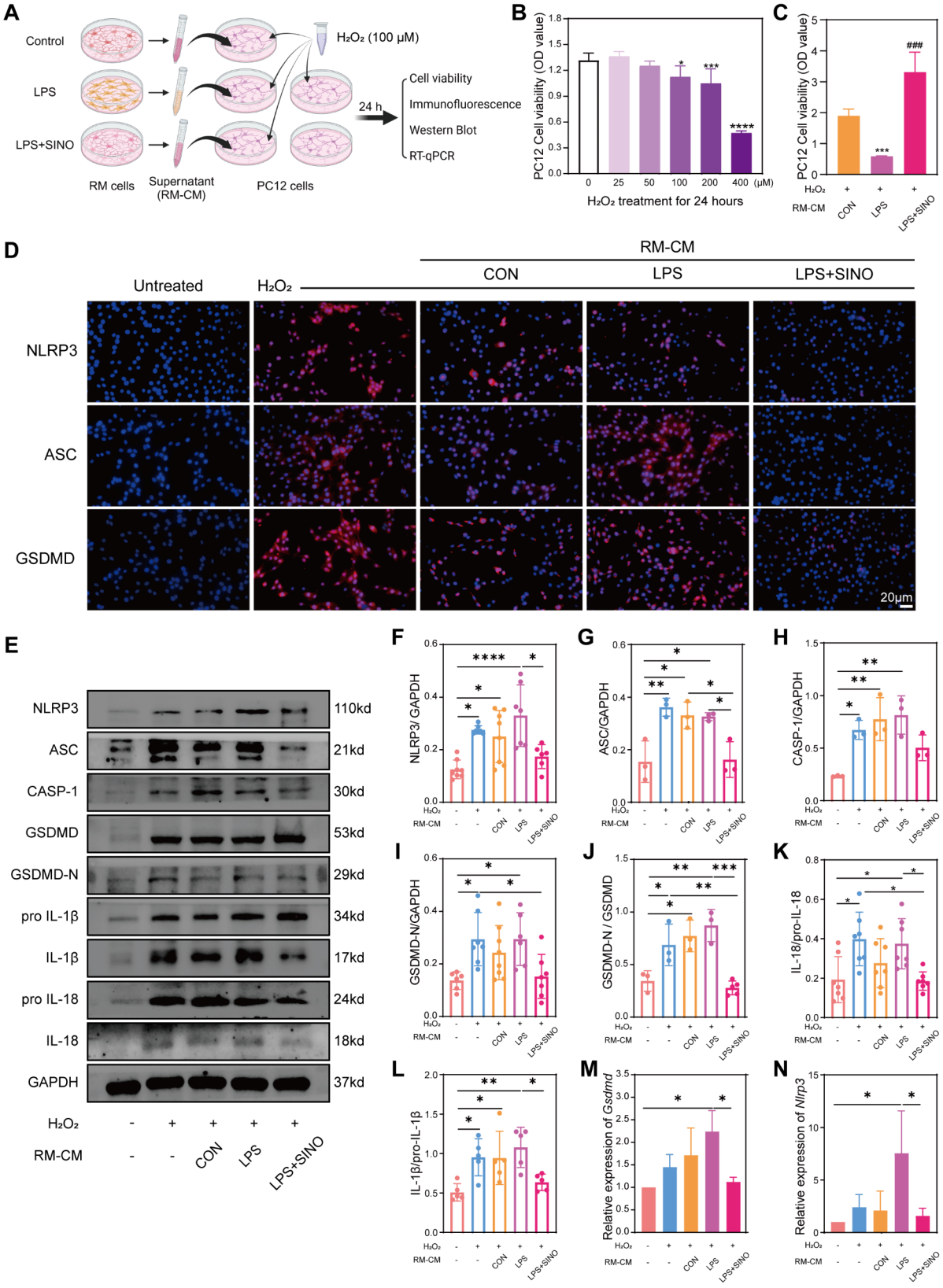

Fig. 5 (See legend on next page.)

(See figure on previous page.)

Fig. 5 SINO-treated RM-CM alleviates H_2O_2-induced PC12 neuronal cell damage and pyroptosis. (**A**) Schematic illustration: Acquisition of RM-CM from different groups and establishment of an in vitro neuronal cell damage model. (**B**) Determination of the optimal concentration of H_2O_2 based on PC12 cell viability. *$P < 0.05$, ***$P < 0.001$, ****$P < 0.0001$ vs. NC. (**C**) SINO-treated RM-CM improved PC12 cell viability. ***$P < 0.001$ vs. the control group. ###$P < 0.001$ vs. the LPS group. (**D**) Immunofluorescence detection of the levels of the pyroptosis-related proteins NLRP3, ASC, and GSDMD in PC12 cells. (**E**) WB analysis of differences in the expression of proteins downstream of NLRP3 in PC12 cells after treatment. (**F**-**L**) Quantitative analysis of the levels of these proteins. (**M**, **N**) RT–qPCR detection of the mRNA expression levels of *Nlrp3* and *Gsdmd* in PC12 cells. *$P < 0.05$, **$P < 0.01$, ***$P < 0.001$ and ****$P < 0.0001$. $n \geq 3$ per group

20 differentially expressed miRNAs were identified in the sequencing results, with 11 upregulated and 9 downregulated miRNAs, based on a fold change ≥ 2 and a P value < 0.05 (Fig. 7D and E, Table S4). miR-223-3p, which was found to be highly upregulated in SINO-RM-Exos, was identified as a potential regulator of NLRP3 expression (Fig. 7F, G). This suggests that miR-223-3p might play a crucial role in modulating neuroinflammation and pyroptosis in neurons.

To further investigate the effect of RM-derived exosomal miR-223-3p in H_2O_2-induced PC12 cells, we conducted transfection experiments. The expression of miR-223-3p in RM cells was significantly upregulated by the miR-223-3p mimic but was significantly downregulated by the miR-223-3p inhibitor (Fig. 7H). The corresponding RM-CM was collected to treat H_2O_2-treated PC12 cells separately. The PCR results showed that the miR-223-3p mimic significantly suppressed *Nlrp3* expression, while the miR-223-3p inhibitor significantly increased *Nlrp3* expression (Fig. 7I). Subsequently, we treated H_2O_2-treated PC12 cells with SINO-RM-Exos and miR-223-3p inhibitor. The findings showed that SINO-RM-Exos efficiently suppressed the expression of *Nlrp3* in PC12 cells. However, the miR-223-3p inhibitor reversed this effect and upregulated the expression of *Nlrp3* (Fig. 7J). Immunofluorescence and WB analysis revealed that treatment with SINO-RM-Exos significantly decreased the protein levels of NLRP3, ASC, and GSDMD in PC12 cells. However, this protective effect was reversed by the miR-223-3p inhibitor (Fig. 7K-O). In conclusion, RM exosomes processed by SINO inhibit NLRP3-mediated pyroptosis in PC12 cells through the transfer of miR-223-3p.

Discussion

In the intricate pathological cascade of CCH, inflammation plays a dual role and is essential for brain tissue repair while also acting as a significant contributor to secondary brain injury. Consequently, modulating neuroinflammation and mitigating neuronal damage have emerged as pivotal strategies for CCH treatment [7, 54]. Through our investigation employing SINO treatment in CCH-afflicted rats, we made several noteworthy observations. First, SINO effectively alleviated brain damage and notably ameliorated cognitive dysfunction in CCH rats. Second, SINO exerted its anti-inflammatory effects by modulating the polarization of microglia, shifting their phenotype from the proinflammatory M1 state to the anti-inflammatory M2 state. Finally, M2 microglia release exosomes that facilitate the delivery of miR-223-3p to target and downregulate *Nlrp3* expression in neuronal cells, thereby suppressing pyroptosis and fostering neural functional recovery. This study offers insights into the role and mechanism of SINO in CCH and provides robust evidence for its clinical application in treatment (Fig. 8).

With a large amount of domestic and foreign basic and clinical research, it has been discovered that SINO possesses a wide range of pharmacological activities, including anti-inflammatory, immunosuppressive, antitumor, and antiarrhythmic effects. Additionally, it plays a crucial neuroprotective role within the central nervous system [11, 20]. However, the role of SINO in CCH remains uncertain. We utilized a widely accepted BCCAO-induced CCH rat model and administered SINO via intraperitoneal injection [46]. The experimental results (Fig. 1) demonstrated that SINO significantly enhanced brain injury recovery and improved learning and memory abilities in CCH rats, which is consistent with previous findings.

Based on the findings above and reports of the anti-inflammatory properties of SINO, we conducted a comprehensive investigation on the anti-inflammatory effects of SINO in CCH. Ni et al. reported that the SINO derivative C16 can reprogram macrophages from the M1 to the M2 phenotype, possibly by mediating the p-p38/p-AKT or STAT1 signaling pathway [25]. Shukla et al. discovered that SINO could inhibit amyloid-β (Aβ)-induced microglial activation and protect hippocampal cells from neurotoxicity in the treatment of AD [40]. Moreover, SINO can inhibit the activity of nicotinamide adenine dinucleotide phosphate (NADPH) oxidase and inhibit the production of various proinflammatory mediators by activated microglia [31]. In addition, SINO can enhance the M2 phenotype of microglia and mitigate inflammatory injury in cerebral hemorrhage [39]. Therefore, we hypothesize that SINO may regulate microglial cell polarization to alleviate CCH-induced neuroinflammation. As expected, following SINO treatment, there was a significant decrease in the mRNA expression and protein levels of the M1 phenotype marker INOS in CCH rat brain tissue samples. The expressions of the proinflammatory factors IL-1β and IL-18 were also distinctly decreased. Conversely, there was an increase in both

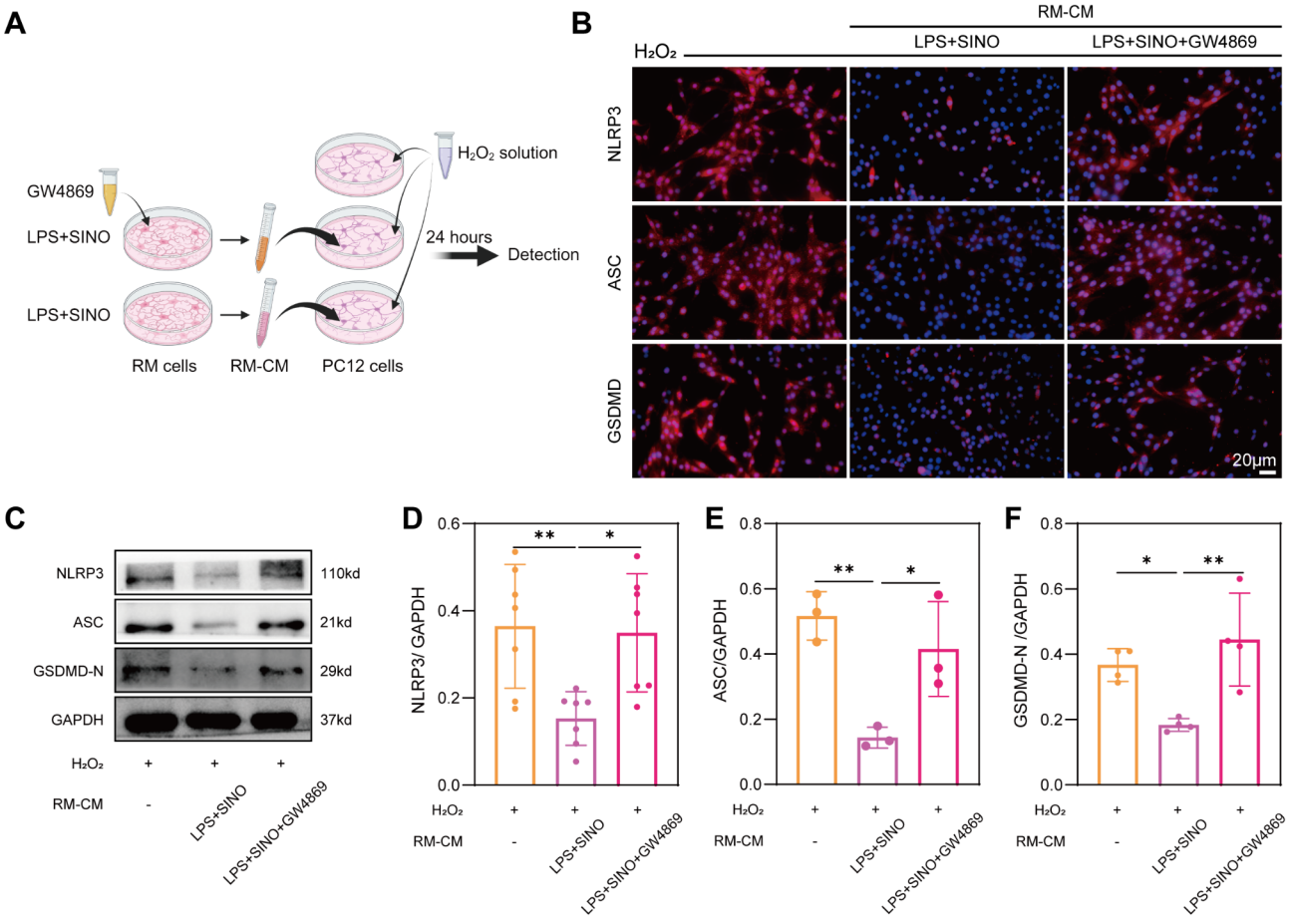

Fig. 6 Exploration of the effects of RM cell exosomes on H_2O_2-induced pyroptosis in PC12 cells. (**A**) Schematic diagram showing the treatment of PC12 cells with RM-CM cocultured with SINO and with or without GW4869. (**B**) Immunofluorescence analysis of pyroptosis-related protein levels in H_2O_2-treated PC12 cells treated with RM-CM with or without inhibition of exosome secretion. (**C**-**F**) WB analysis of the protein levels of NLRP3, ASC, and GSDMD-N. $^*P < 0.05$ and $^{**}P < 0.01$. $n \geq 3$ per group

the mRNA and protein expression of the M2 phenotype marker ARG-1. The levels of the anti-inflammatory factors IL-4 and IL-10 were increased (Fig. 2). This finding suggested that SINO may play an important role in anti-inflammatory responses by regulating M1 to M2 microglial polarization.

Numerous studies have demonstrated that inflammation triggers a form of programmed cell death known as pyroptosis. In nervous system diseases, inflammation promotes the activation of the NLRP3 inflammasome, leading to neuronal pyroptosis and subsequent brain injury and cognitive impairment [9, 53]. The process of pyroptosis involves the stimulation of pattern recognition receptors (PPRs), the formation of inflammasomes, the activation of caspase proteins, the activation of gasdermin D (GSDMD), the bursting of cell membranes, and the release of inflammatory factors. Stimulation of the PPR by pathogen-associated molecular patterns (PAMPs) or damage-associated molecular patterns (DAMPs) leads to the activation of inflammasomes [18, 24]. Typical inflammasomes are macromolecular protein complexes composed of sensors (mainly NLR family proteins and PYHIN family proteins), the adapter ASC, and effectors, including NLRP1, NLRP3, NAIP-NLRC4, and AIM. Among them, the NLRP3 inflammasome is the most characteristic and extensively studied [28]. Activated NLRP3 binds to ASCs and recruits pro-caspase-1 to form an inflammasome [12]. The formation of inflammasomes leads to the transformation of pro-caspase-1 into activated caspase-1, which is capable of cleaving pro-IL-1β, pro-IL-18, and GSDMD to generate bioactive IL-1β, IL-18, and N-terminal gasdermin-D (GSDMD-N). GSDMD-N can penetrate the cell membrane, forming a pore that leads to the forced uptake of external ions and water, cellular swelling, rapid cell lysis, and the release of cellular contents such as the inflammatory factors IL-1β and IL-18, ultimately exacerbating inflammation [22]. In this study, we found that the mRNA expression of *Nlrp3* and *Gsdmd* increased in CCH rat brain tissue, accompanied by increased protein levels of NLRP3, ASC,

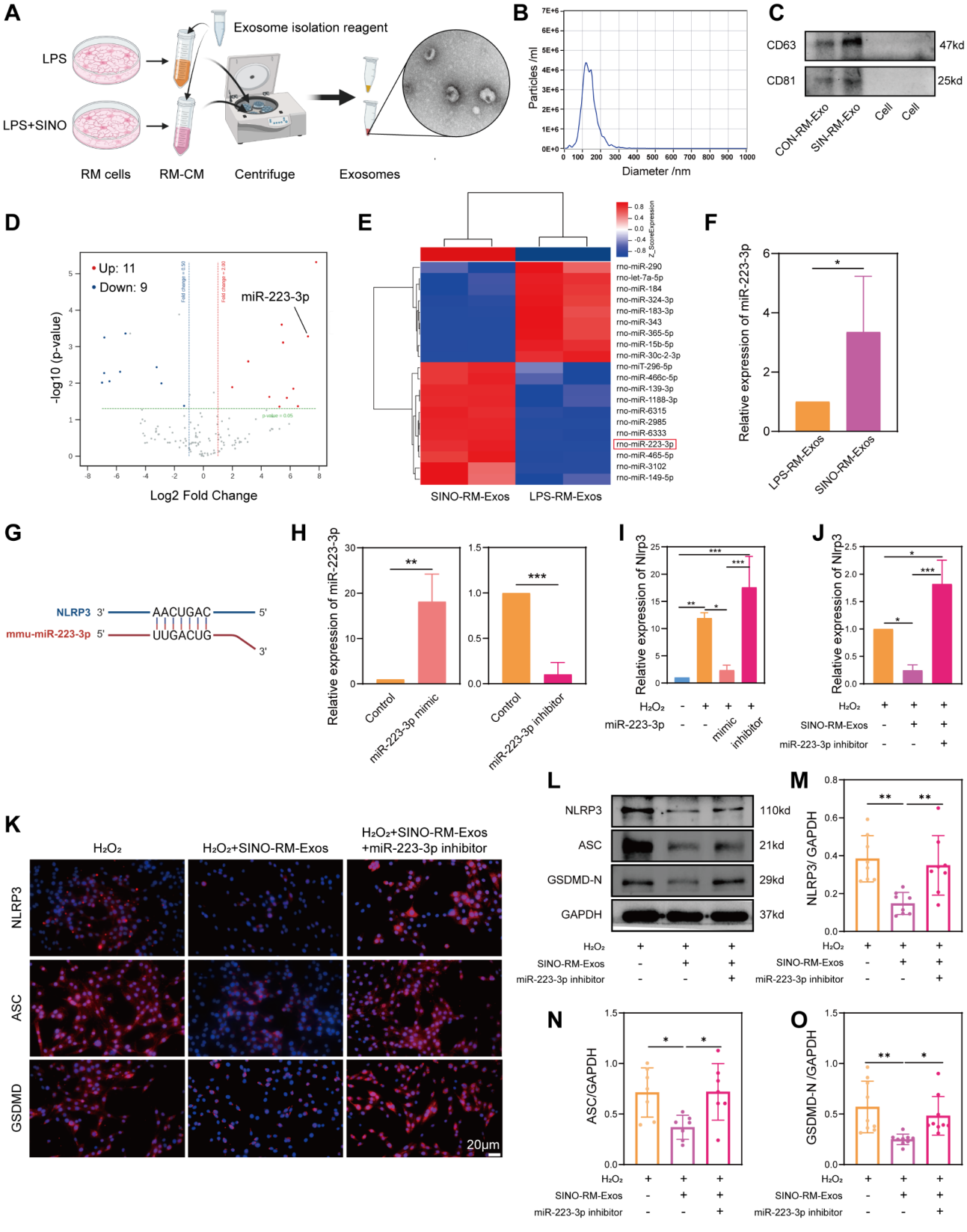

Fig. 7 (See legend on next page.)

(See figure on previous page.)

Fig. 7 SINO-treated RM cell-derived exosomes inhibit NLRP3-mediated pyroptosis in PC12 cells via miR-223-3p. (**A**, **B**) Isolation and identification of exosomes from RM cells (RM-Exos). The morphology and particle size of the exosomes were identified through transmission electron microscopy and nanoparticle tracking analysis. (**C**) The levels of the exosome marker proteins CD63 and CD81 were determined via WB analysis. (**D**, **E**) Volcano plot and heatmap illustrating the differentially expressed miRNAs in the CON-RM-EXO and SINO-RM-EXO groups determined by miRNA sequencing. (**F**) RT–qPCR validation of the differential expression of exosomal miR-223-3p. (**G**) The targeted binding relationship between miR-223-3p and *Nlrp3*. (**H**) miR-223-3p expression in RM cells after transfection with the miR-223-3p mimic or inhibitor. (**I**) The expression of the target mRNA *Nlrp3* in PC12 cells was measured after treatment with RM-CM transfected with the miR-223-3p mimic and inhibitor. (**J**) The miR-223-3p inhibitor reversed the downregulation of *Nlrp3* in PC12 cells induced by SINO-RM-Exos. (**K**) Immunofluorescence observation of the effects of SINO-RM-Exos transfected with the miR-223-3p inhibitor on pyroptosis-related proteins in PC12 cells. (**L**-**O**) Detection of the protein levels of NLRP3, ASC, and GSDMD-N in PC12 cells by WB analysis. *$P < 0.05$, **$P < 0.01$, and ***$P < 0.001$. $n \geq 3$ per group

CASP-1, GSDMD-N, IL-1β and IL-18 (Fig. 3). These findings suggest that inflammation triggers the activation of the NLRP3 inflammasome in CCH, resulting in neuronal pyroptosis. Importantly, SINO treatment prevents this phenomenon.

Exosomes, as important mediators of intercellular communication, play a key role in physiological and pathological processes. It can carry a variety of signaling molecules, including proteins, lipids, cytokines, mRNAs, and miRNAs [43]. Studies have shown that microglial exosomes play an important role in mediating the interaction between microglia and neurons [4, 27]. As anti-inflammatory agents, M2 microglia-derived exosomes can reduce neuronal responses to cerebral ischemia damage after they are internalized by neurons [41, 52]. Chen et al. effectively improved cognitive function in AD mice using exosomes secreted by M2 microglia induced by near-infrared light [5]. Therefore, this study further explored the effect of SINO treatment on microglial exosomes in CCH. First, we established an inflammation model in RM cells by LPS induction and observed that RM cells polarized to the M1 phenotype. However, after SINO treatment, the RM cells polarized to the M2 phenotype, which was consistent with the results of the animal experiments (Fig. 4). Subsequently, we collected the supernatant of RM cells treated with SINO as a conditioned medium for treating H_2O_2-treated PC12 cells. The results demonstrated that CM derived from SINO-treated RM cells effectively inhibited pyroptosis in PC12 cells, but this effect was counteracted by the addition of the exosome inhibitor GW4869 (Figs. 5 and 6). This indicates that exosomes released by SINO-induced M2 polarization of RM cells inhibited pyroptosis in PC12 cells.

Recently, an increasing number of studies have shown that exosomal miRNAs, as key functional elements of intercellular interactions, play important roles in regulating brain injury [19, 51]. MiRNAs, a type of small non-coding RNA molecule, recognize the 3'UTR of target genes through complementary base pairing and guide the silencing complex to degrade target gene mRNA or inhibit its translation according to the degree of complementarity [38]. MicroRNAs (miRNAs) derived from microglial exosomes can alleviate neurological damage in acute brain injury and neurodegenerative disease through different pathways, thereby improving neurological function [5, 10, 41, 52]. In this study, to further explore the molecular mechanism by which SINO-treated RM cell exosomes (SINO-RM-Exos) regulate PC12 cell pyroptosis, we isolated RM exosomes with or without SINO treatment for miRNA sequencing and identified 11 miRNAs that were significantly upregulated in the SINO-RM-Exos (Fig. 7, Table S4). These findings were verified using qRT−PCR analysis. We discovered that miRNA-223-3p can target and bind to the NLRP3 gene, leading to anti-inflammatory and antipyroptotic effects. The remaining 10 upregulated miRNAs—miR-296-5p, miR-139-3p, miR-466c-5p, miR-465-5p, miR-1188-3p, miR-2985, miR-6315, miR-3102, miR-6333, and miR-149-5p—are rarely reported in the nervous system. Therefore, they were excluded from the focus of our study. As depicted in Fig. 7, treatment with SINO-RM-Exos significantly suppressed *Nlrp3* mRNA expression in H_2O_2-treated PC12 cells and downregulated the protein levels of NLRP3, ASC, and GSDMD. However, after transfection of the miR-223-3p inhibitor, this effect was significantly weakened. These results suggested that SINO-RM-Exos could inhibit the transcription and translation of NLRP3 by delivering miR-223-3p, thereby alleviating pyroptosis in PC12 cells. While our study focused on the neuroprotective effects of exosomal miR-223-3p, which was found to inhibit NLRP3-mediated neuronal pyroptosis, it is important to note that exosomes can also propagate neuroinflammation. These vesicles carry a variety of molecules, including pro-inflammatory cytokines, damage-associated molecular patterns (DAMPs), and microRNAs, which can further activate glial cells or neurons in the surrounding tissue, thereby exacerbating inflammation. This dual role of exosomes—both as mediators of neuroinflammation and as potential regulators of inflammation—warrants further investigation.

Conclusion

In summary, neuroinflammation significantly impacts hippocampal neuros and cognitive function in CCH rats. SINO treatment promotes a shift in microglial

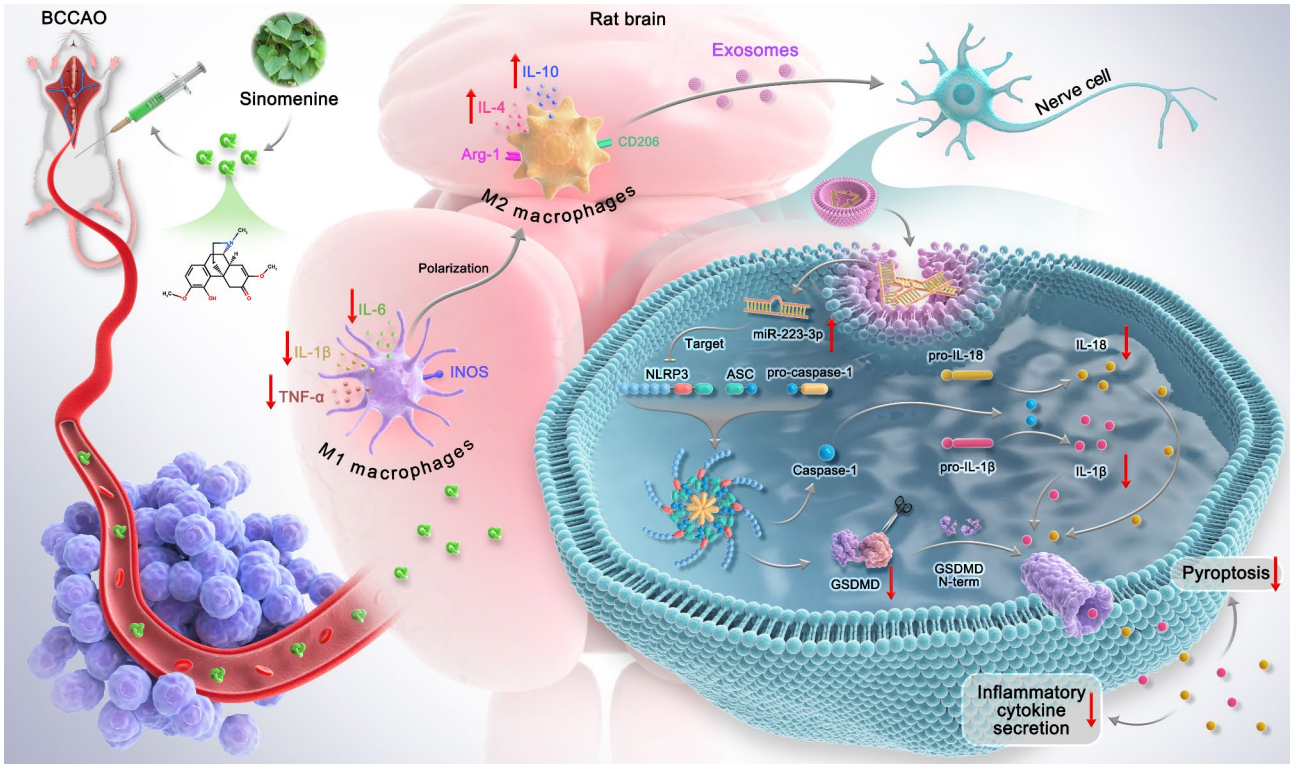

Fig. 8 The mechanism diagram illustrating how SINO improves neuroinflammation, neuronal cell damage, and pyroptosis in CCH rats. SINO regulates microglial cell polarization toward the M2 phenotype and promotes the release of exosomes containing miR-223-3p, thereby reducing the inflammatory response and targeting NLRP3-mediated pyroptosis in neuronal cells

polarization from M1 to M2, thereby reducing the inflammatory response. Mechanistically, exosomes derived from SINO-treated microglial deliver miR-223-3p, which inhibits NLRP3/ASC/GSDMD-mediated pyroptosis and neuronal damage (Fig. 8). However, this study has some limitations. Further investigation using a neuron-microglia co-culture model is necessary to explore the cortical therapeutic effects of SINO on inflammation, beyond its impact on the hippocampus. Nevertheless, this research provides valuable insights and a theoretical foundation for the potential use of SINO in treating neuroinflammation.

Abbreviations

ARG-1	Arginase-1
BCCAO	Bilateral common carotid artery occlusion
CASP-1	Caspase-1
CCH	Chronic cerebral hypoperfusion
CM	Conditioned medium
IBA1	Ionized calcium-binding adapter molecule 1
INOS	Inducible NO synthase
IFN-γ	Interferon-γ
MWM	Morris water maze
NLRP3	NOD-like receptor protein 3
GSDMD-N	N-terminal fragment of gasdermin D
RM	Rat microglia
SINO	Sinomenine
TGF-β	Transforming growth factor-β
TNF-α	Tumor necrosis factor-α

Supplementary Information

The online version contains supplementary material available at https://doi.org/10.1186/s40478-025-01950-z .

Supplementary Material 1

Supplementary Material 2

Acknowledgements
Not applicable.

Author contributions
Qu Yang: Conceptualization, Data curation, Methodology, Writing- original draft. Kaibing Zhang: Data curation, Software, Methodology. Qi Chen: Formal Analysis, Validation, Visualization, Writing-review & editing. Yu Liu: Resources, Methodology, Funding acquisition. Jiacheng Zheng: Data curation, Methodology. Dongxia Hu: Supervision, Formal Analysis. Jun Luo: Conceptualization, Funding acquisition, Project administration, Writing-review & editing.

Funding
This work was funded by the Jiangxi Province Key Laboratory of Precision Cell Therapy (No. 2024SSY06241) and the National Natural Science Foundation of China (No. 82360174 to J.L.; No. 32360198 and 82301675 to Y.L.).

Data availability
The datasets supporting the conclusions of this article are available from the corresponding author upon reasonable request.

Declarations

Ethics approval and consent to participate

The Laboratory Animal Science Center of Nanchang University reviewed and approved this study.

Consent for publication

All authors have reviewed the manuscript and consented to its publication. Each author had full access to the study data and assumed responsibility for its integrity and the accuracy of the data analysis.

Competing interests

The authors declare no competing interests.

Received: 20 September 2024 / Accepted: 5 February 2025
Published online: 05 March 2025

References

1. Aires ID, Ribeiro-Rodrigues T, Boia R, Ferreira-Rodrigues M, Girão H, Ambrósio AF, Santiago AR (2021) Microglial extracellular vesicles as vehicles for Neurodegeneration spreading. Biomolecules 11. https://doi.org/10.3390/biom11060770
2. Badji A, Youwakim J, Cooper A, Westman E, Marseglia A (2023) Vascular cognitive impairment - past, present, and future challenges. Ageing Res Rev 90:102042. https://doi.org/10.1016/j.arr.2023.102042
3. Chan KY, Wang W, Wu JJ, Liu L, Theodoratou E, Car J, Middleton L, Russ TC, Deary IJ, Campbell Het al et al (2013) Epidemiology of Alzheimer's disease and other forms of dementia in China, 1990–2010: a systematic review and analysis. Lancet 381:2016–2023. https://doi.org/10.1016/S0140-6736(13)60221-4
4. Chen Y, Zhu J, Ji J, Liu Z, Ren G (2022) The role of microglial exosomes in brain injury. Front Cell Neurosci 16:1003809. https://doi.org/10.3389/fncel.2022.1003809
5. Chen C, Bao Y, Xing L, Jiang C, Guo Y, Tong S, Zhang J, Chen L, Mao Y (2023) Exosomes derived from M2 microglial cells modulated by 1070-nm light improve cognition in an Alzheimer's Disease Mouse Model. Adv Sci (Weinh) 10:e2304025. https://doi.org/10.1002/advs.202304025
6. Cheng C-Y, Barro L, Tsai S-T, Feng T-W, Wu X-Y, Chao C-W, Yu R-S, Chin T-Y, Hsieh MF (2021) Epigallocatechin-3-gallate-loaded liposomes Favor Anti-inflammation of Microglia cells and promote neuroprotection. Int J Mol Sci 22. https://doi.org/10.3390/ijms22063037
7. Choi B, Lee C, Yu J-W (2023) Distinctive role of inflammation in tissue repair and regeneration. Arch Pharm Res 46:78–89. https://doi.org/10.1007/s12272-023-01428-3
8. Dhaliwal N, Dhaliwal J, Singh A, Chopra K (2021) Dimethyl fumarate attenuates 2-VO-induced vascular dementia via activating the Nrf2 signaling pathway in rats. Inflammopharmacology 29:537–547. https://doi.org/10.1007/s10787-020-00785-5
9. Ding R, Li H, Liu Y, Ou W, Zhang X, Chai H, Huang X, Yang W, Wang Q (2022) Activating cGAS-STING axis contributes to neuroinflammation in CVST mouse model and induces inflammasome activation and microglia pyroptosis. J Neuroinflamm 19:137. https://doi.org/10.1186/s12974-022-02511-0
10. Ge X, Guo M, Hu T, Li W, Huang S, Yin Z, Li Y, Chen F, Zhu L, Kang C al (2020) Increased Microglial Exosomal Mir-124-3p alleviates neurodegeneration and improves cognitive outcome after rmTBI. Mol Ther 28:503–522. https://doi.org/10.1016/j.ymthe.2019.11.017
11. Hong H, Lu X, Lu Q, Huang C, Cui Z (2022) Potential therapeutic effects and pharmacological evidence of sinomenine in central nervous system disorders. Front Pharmacol 13:1015035. https://doi.org/10.3389/fphar.2022.1015035
12. Hu HL, Bennett N, Holton JL, Nolan CC, Lister T, Cavanagh JB, Ray DE (1999) Glutathione depletion increases brain susceptibility to m-dinitrobenzene neurotoxicity. Neurotoxicology 20:83–90
13. Huang Y, Xu W, Zhou R (2021) NLRP3 inflammasome activation and cell death. Cell Mol Immunol 18:2114–2127. https://doi.org/10.1038/s41423-021-00740-6
14. Jha MK, Lee W-H, Suk K (2016) Functional polarization of neuroglia: implications in neuroinflammation and neurological disorders. Biochem Pharmacol 103. https://doi.org/10.1016/j.bcp.2015.11.003
15. Jiang T, Zhang L, Pan X, Zheng H, Chen X, Li L, Luo J, Hu X (2017) Physical Exercise improves cognitive function together with Microglia phenotype modulation and remyelination in chronic cerebral hypoperfusion. Front Cell Neurosci 11:404. https://doi.org/10.3389/fncel.2017.00404
16. Kalaria RN, Maestre GE, Arizaga R, Friedland RP, Galasko D, Hall K, Luchsinger JA, Ogunniyi A, Perry EK, Potocnik F al (2008) Alzheimer's disease and vascular dementia in developing countries: prevalence, management, and risk factors. Lancet Neurol 7:812–826. https://doi.org/10.1016/S1474-4422(08)70169-8
17. Kang YJ, Tan H-Y, Lee CY, Cho H (2021) An Air Particulate Pollutant induces Neuroinflammation and Neurodegeneration in Human Brain models. Adv Sci (Weinh) 8:e2101251. https://doi.org/10.1002/advs.202101251
18. Lamkanfi M, Dixit VM (2014) Mechanisms and functions of inflammasomes. Cell 157:1013–1022. https://doi.org/10.1016/j.cell.2014.04.007
19. Li S, Lv D, Yang H, Lu Y, Jia Y (2023) A review on the current literature regarding the value of exosome miRNAs in various diseases. Ann Med 55:2232993. https://doi.org/10.1080/07853890.2023.2232993
20. Li D, Zhong Z, Ko C-N, Tian T, Yang C (2023) From mundane to classic: Sinomenine as a multi-therapeutic agent. Br J Pharmacol. https://doi.org/10.1111/bph.16267
21. Li J-M, Yao Y-D, Luo J-F, Liu J-X, Lu L-L, Liu Z-Q, Dong Y, Xie Y, Zhou H (2023) Pharmacological mechanisms of sinomenine in anti-inflammatory immunity and osteoprotection in rheumatoid arthritis: a systematic review. Phytomedicine 121:155114. https://doi.org/10.1016/j.phymed.2023.155114
22. Liu X, Zhang Z, Ruan J, Pan Y, Magupalli VG, Wu H, Lieberman J (2016) Inflammasome-activated gasdermin D causes pyroptosis by forming membrane pores. Nature 535:153–158. https://doi.org/10.1038/nature18629
23. Liu W, Zhang Y, Zhu W, Ma C, Ruan J, Long H, Wang Y (2018) Sinomenine inhibits the progression of rheumatoid arthritis by regulating the secretion of inflammatory cytokines and Monocyte/Macrophage subsets. Front Immunol 9:2228. https://doi.org/10.3389/fimmu.2018.02228
24. Lu F, Lan Z, Xin Z, He C, Guo Z, Xia X, Hu T (2020) Emerging insights into molecular mechanisms underlying pyroptosis and functions of inflammasomes in diseases. J Cell Physiol 235:3207–3221. https://doi.org/10.1002/jcp.29268
25. Ni P, Liu Y-Q, Man J-Y, Li W, Xue S-S, Lu T-H, Su Z-L, Zhou C-L (2021) C16, a novel sinomenine derivatives, promoted macrophage reprogramming toward M2-like phenotype and protected mice from endotoxemia. Int J Immunopathol Pharmacol 35:20587384211026786. https://doi.org/10.1177/20587384211026786
26. O'Brien JT, Thomas A (2015) Vascular dementia. Lancet 386:1698–1706. https://doi.org/10.1016/S0140-6736(15)00463-8
27. Panaro MA, Benameur T, Porro C (2020) Extracellular vesicles miRNA Cargo for Microglia polarization in traumatic brain Injury. Biomolecules 10. https://doi.org/10.3390/biom10060901
28. Patel MN, Carroll RG, Galván-Peña S, Mills EL, Olden R, Triantafilou M, Wolf AI, Bryant CE, Triantafilou K, Masters SL (2017) Inflammasome priming in sterile inflammatory disease. Trends Mol Med 23:165–180. https://doi.org/10.1016/j.molmed.2016.12.007
29. Perry VH, Holmes C (2014) Microglial priming in neurodegenerative disease. Nat Rev Neurol 10:217–224. https://doi.org/10.1038/nrneurol.2014.38
30. Poh L, Sim WL, Jo D-G, Dinh QN, Drummond GR, Sobey CG, Chen CL-H, Lai MKP, Fann DY, Arumugam TV (2022) The role of inflammasomes in vascular cognitive impairment. Mol Neurodegeneration 17:4. https://doi.org/10.1186/s13024-021-00506-8
31. Qian L, Xu Z, Zhang W, Wilson B, Hong J-S, Flood PM (2007) Sinomenine, a natural dextrorotatory morphinan analog, is anti-inflammatory and neuroprotective through inhibition of microglial NADPH oxidase. J Neuroinflamm 4:23
32. Qiu J, Wang M, Zhang J, Cai Q, Lu D, Li Y, Dong Y, Zhao T, Chen H (2016) The neuroprotection of sinomenine against ischemic stroke in mice by suppressing NLRP3 inflammasome via AMPK signaling. Int Immunopharmacol 40:492–500. https://doi.org/10.1016/j.intimp.2016.09.024
33. Qiu J, Yan Z, Tao K, Li Y, Li Y, Li J, Dong Y, Feng D, Chen H (2016) Sinomenine activates astrocytic dopamine D2 receptors and alleviates neuroinflammatory injury via the CRYAB/STAT3 pathway after ischemic stroke in mice. J Neuroinflamm 13:263
34. Rajeev V, Chai YL, Poh L, Selvaraji S, Fann DY, Jo D-G, De Silva TM, Drummond GR, Sobey CG, Arumugam TV al (2023) Chronic cerebral hypoperfusion: a critical feature in unravelling the etiology of vascular cognitive impairment. Acta Neuropathol Commun 11:93. https://doi.org/10.1186/s40478-023-01590-1

35. Ransohoff RM (2016) How neuroinflammation contributes to neurodegeneration. Sci (New York NY) 353:777–783. https://doi.org/10.1126/science.aag2590
36. Rey C, Nadjar A, Buaud B, Vaysse C, Aubert A, Pallet V, Layé S, Joffre C (2016) Resolvin D1 and E1 promote resolution of inflammation in microglial cells in vitro. Brain Behav Immun 55:249–259. https://doi.org/10.1016/j.bbi.2015.12.013
37. Schroder K, Tschopp J (2010) The inflammasomes. Cell 140:821–832. https://doi.org/10.1016/j.cell.2010.01.040
38. Shang R, Lee S, Senavirathne G, Lai EC (2023) microRNAs in action: biogenesis, function and regulation. Nat Rev Genet 24:816–833. https://doi.org/10.1038/s41576-023-00611-y
39. Shi H, Zheng K, Su Z, Su H, Zhong M, He X, Zhou C, Chen H, Xiong Q, Zhang Y (2016) Sinomenine enhances microglia M2 polarization and attenuates inflammatory injury in intracerebral hemorrhage. J Neuroimmunol 299:28–34. https://doi.org/10.1016/j.jneuroim.2016.08.010
40. Shukla SM, Sharma SK (2011) Sinomenine inhibits microglial activation by Aβ and confers neuroprotection. J Neuroinflamm 8:117. https://doi.org/10.1186/1742-2094-8-117
41. Song Y, Li Z, He T, Qu M, Jiang L, Li W, Shi X, Pan J, Zhang L, Wang Y al (2019) M2 microglia-derived exosomes protect the mouse brain from ischemia-reperfusion injury via exosomal miR-124. Theranostics 9:2910–2923. https://doi.org/10.7150/thno.30879
42. Su L, Li R, Zhang Z, Liu J, Du J, Wei H (2022) Identification of altered exosomal microRNAs and mRNAs in Alzheimer's disease. Ageing Res Rev 73:101497. https://doi.org/10.1016/j.arr.2021.101497
43. Tenchov R, Sasso JM, Wang X, Liaw W-S, Chen C-A, Zhou QA (2022) ExosomesNature's lipid nanoparticles, a rising star in Drug Delivery and Diagnostics. ACS Nano 16:17802–17846. https://doi.org/10.1021/acsnano.2c08774
44. Tian Y, Zhu P, Liu S, Jin Z, Li D, Zhao H, Zhu X, Shu C, Yan D, Dong Z (2019) IL-4-polarized BV2 microglia cells promote angiogenesis by secreting exosomes. Adv Clin Exp Med 28:421–430. https://doi.org/10.17219/acem/91826
45. Trotta T, Panaro MA, Cianciulli A, Mori G, Di Benedetto A, Porro C (2018) Microglia-derived extracellular vesicles in Alzheimer's Disease: a double-edged sword. Biochem Pharmacol 148:184–192. https://doi.org/10.1016/j.bcp.2017.12.020
46. Washida K, Hattori Y, Ihara M (2019) Animal models of chronic cerebral hypoperfusion: from mouse to Primate. Int J Mol Sci 20. https://doi.org/10.3390/ijms20246176
47. WHO (2021) Global status report on the public health response to dementia. World Health Organization, Geneva.
48. Yang Z, Liu Y, Yuan F, Li Z, Huang S, Shen H, Yuan B (2014) Sinomenine inhibits microglia activation and attenuates brain injury in intracerebral hemorrhage. Mol Immunol 60:109–114. https://doi.org/10.1016/j.molimm.2014.03.005
49. Yang T, Sun Y, Lu Z, Leak RK, Zhang F (2017) The impact of cerebrovascular aging on vascular cognitive impairment and dementia. Ageing Res Rev 34:15–29. https://doi.org/10.1016/j.arr.2016.09.007
50. Yao Y, Jiang Y, Song J, Wang R, Li Z, Yang L, Wu W, Zhang L, Peng Q (2023) Exosomes as potential functional nanomaterials for tissue Engineering. Adv Healthc Mater 12:e2201989. https://doi.org/10.1002/adhm.202201989
51. Zhang J, Li S, Li L, Li M, Guo C, Yao J, Mi S (2015) Exosome and exosomal microRNA: trafficking, sorting, and function. Genomics Proteom Bioinf 13:17–24. https://doi.org/10.1016/j.gpb.2015.02.001
52. Zhang D, Cai G, Liu K, Zhuang Z, Jia K, Pei S, Wang X, Wang H, Xu S, Cui C al (2021) Microglia exosomal miRNA-137 attenuates ischemic brain injury through targeting Notch1. Aging 13:4079–4095. https://doi.org/10.18632/aging.202373
53. Zhang Y, Zhang J, Zhao Y, Zhang Y, Liu L, Xu X, Wang X, Fu J (2023) ChemR23 activation attenuates cognitive impairment in chronic cerebral hypoperfusion by inhibiting NLRP3 inflammasome-induced neuronal pyroptosis. Cell Death Dis 14:721. https://doi.org/10.1038/s41419-023-06237-6
54. Zheng Y, Zhang J, Zhao Y, Zhang Y, Zhang X, Guan J, Liu Y, Fu J (2021) Curcumin protects against cognitive impairments in a rat model of chronic cerebral hypoperfusion combined with diabetes mellitus by suppressing neuroinflammation, apoptosis, and pyroptosis. Int Immunopharmacol 93:107422. https://doi.org/10.1016/j.intimp.2021.107422

Publisher's note